Self-interaction free local exchange potentials applied to metallic systems

S. J. Clark[1], T. W. Hollins[1], K. Refson[2] and N. I. Gidopoulos[1]

[1]Department of Physics, Durham University, South Road, Durham, DH1 3LE, United Kingdom.

[2]Department of Physics, Royal Holloway University of London, United Kingdom and Science and Technology Facilities Council, Rutherford Appleton Laboratory, Didcot, Oxfordshire OX11 0QX, England, United Kingdom

Abstract. We extend the formalism of local exchange methods to calculate and investigate the electronic structure of metals. It is well-known that the Hartree-Fock method when applied to metals shows unphysical behaviour, however the accurate treatment of exchange via DFT's exact exchange method (EXX) and using our local Fock exchange method (LFX) can be used to describe metallic band structures accurately.

PACS numbers:

1. Introduction

Prevention is a better than cure and the best way to avoid self interaction errors in electronic structure calculations must be the accurate treatment of exchange. In Hartree-Fock (HF) theory (often referred to as "exact exchange"), exchange effects are indeed treated accurately (or exactly) but only for orbitals occupied in the ground state HF Slater determinant. As is well known[1] the HF single-particle operator treats in an asymmetric way its eigenfunctions representing occupied orbitals in the HF Slater determinant, from its eigenfunctions that represent virtual orbitals. For an N electron system, each occupied orbital is repelled by the charge of $N-1$ electrons, while the unoccupied orbitals are repelled by the full charge of N electrons. If we view a HF virtual orbital, ϕ_a, as a single-particle excitation from a ground state occupied orbital, ϕ_i, then this asymmetry is responsible for the self-interaction[2] of the electron hosted in ϕ_a with itself in ϕ_i, i.e. when it occupied the ground state orbital ϕ_i before excitation. This self-interaction is similar to the ghost self-interaction described in Reference [3].

There have been attempts to cure this asymmetry of the HF nonlocal exchange operator, for example by improving the method for generating exchange potentials from electronic wavefunctions[4]. The exact exchange (EXX) approach in DFT and the local Fock exchange (LFX) potential method[5] offer an elegant way to deal with self-interactions in general but in particular with this special case of self-interactions too. They do so by adopting a local exchange potential, which is necessarily common for all eigenorbitals (occupied and virtual) of the single-particle Hamiltonian.

The optimised effective potential (OEP) theory and the EXX potential have been reviewed in detailed elsewhere[6], particularly for non-metals, therefore we briefly mention only a few important works. It has been difficult to obtain a robust method of convergence. The work of Görling *et al* [7, 8] has shown success in this area, compared EXX to Kohn-Sham methods[9] and examined all-electron versus pseudopotential methods[10]. Engel *et al* have examined relativistic OEP methods[11] and extensions of OEP to correlation[12, 13]. Comparisons between exact and semi-local exchange potentials in insulating solids have also been made[15, 14]. Using the OEP is has also been possible to correct for the effect of self-interaction errors in the Kohn-Sham potential[16, 17]. Also, we presented a robust implementation in a plane wave code in two previous publications[5, 21]. Here we extend these methods to the treatment of metals, where convergence is more challenging but our methods are also found to be similarly robust. We are aware of some earlier attempt of exact exchange for metals by Kotani *et al*[18, 19, 20].

In a previous publication we introduced a method to calculate the exact exchange (EXX) potential using perturbation theory[21]. This perturbation theory based method requires us to consider only the N occupied orbitals in the calculation and optimises the Kohn-Sham (KS) effective potential, $v^{\sigma}_{Hx}(\mathbf{r})$, by direct variation of this potential

$$v^{\sigma}_{Hx} \rightarrow v^{\sigma}_{Hx}(\mathbf{r}) - \lambda \delta v^{\sigma}(\mathbf{r}), \tag{1}$$

where $\lambda > 0$. In EXX, the *local* effective potential is the one which minimises the

Hartree-Fock (HF) total energy,

$$E[v^{\sigma}_{Hx}] = \sum_{\sigma}\sum_{i=1}^{N^{\sigma}} -\frac{1}{2}\langle\phi^{\sigma}_{i}|\nabla^{2}|\phi^{\sigma}_{i}\rangle + \int d\mathbf{r} v_{ext}(\mathbf{r})\rho(\mathbf{r}) + \frac{1}{2}\int\int d\mathbf{r}d\mathbf{r}'\frac{\rho(\mathbf{r})\rho(\mathbf{r}')}{|\mathbf{r}-\mathbf{r}'|} - \frac{1}{2}\sum_{\sigma}\sum_{i=1}^{N^{\sigma}}\sum_{j=1}^{N^{\sigma}}\int\int d\mathbf{r}d\mathbf{r}'\frac{\phi^{\dagger\sigma}_{j}(\mathbf{r})\phi^{\sigma}_{i}(\mathbf{r})\phi^{\dagger\sigma}_{i}(\mathbf{r}')\phi^{\sigma}_{j}(\mathbf{r}')}{|\mathbf{r}-\mathbf{r}'|}, \quad (2)$$

where the symbols have their standard meanings and the orbitals, ϕ^{σ}_{i}, are generated from the KS equations

$$\left[-\frac{\nabla^{2}}{2} + v_{ext}(\mathbf{r}) + v^{\sigma}_{Hx}(\mathbf{r})\right]\phi^{\sigma}_{i}(\mathbf{r}) = \varepsilon^{\sigma}_{i}\phi^{\sigma}_{i}(\mathbf{r}). \quad (3)$$

In Eqn(2) we use the usual HF expression for exchange, although an alternative definition in metals can be expressed within the adiabatic connection fluctuation-dissipation theory framework[22].

For completeness, we summarise the method of solution here: the effective potential, $v^{\sigma}_{Hx}(\mathbf{r})$ is found by variational minimisation of the Hartree-Fock (HF) total energy and the potential is updated using the change in the potential, $\delta v^{\sigma}(\mathbf{r})$ given by

$$\delta v^{\sigma}(\mathbf{r}) = \int d\mathbf{r}'\frac{1}{|\mathbf{r}-\mathbf{r}'|}\frac{\delta E[v^{\sigma}_{Hx}]}{\delta v^{\sigma}_{Hx}(\mathbf{r}')}. \quad (4)$$

The functional derivative of the total energy with respect to the potential is

$$\frac{\delta E[v^{\sigma}_{Hx}]}{\delta v^{\sigma}_{Hx}(\mathbf{r}')} = -\sum_{i=1}^{N^{\sigma}}\tilde{\phi}^{\dagger\sigma}_{i}(\mathbf{r})\phi^{\sigma}_{i}(\mathbf{r}) + \text{h.c}, \quad (5)$$

$\tilde{\phi}^{\sigma}_{i}(\mathbf{r})$ is the first order correction to an orbital, explicitly given by

$$\tilde{\phi}^{\sigma}_{i}(\mathbf{r}) = -\sum_{a=N^{\sigma}+1}^{\infty}\frac{\phi^{\sigma}_{a}(\mathbf{r})\langle\phi^{\sigma}_{a}|v_{H}+V^{\sigma}_{x}-v_{Hx}|\phi^{\sigma}_{i}\rangle}{\varepsilon^{\sigma}_{a}-\varepsilon^{\sigma}_{i}}. \quad (6)$$

V_x is the Fock non-local exchange operator. In practice this infinite sum is slowly convergent and numerical attempts at direct solution are plagued with numerical instabilities. For this reason we tackled this problem using a different approach, by calculating the perturbative corrections from the Sternheimer equation

$$(h^{\sigma}-\varepsilon^{\sigma}_{i})|\tilde{\phi}^{\sigma}_{i}\rangle + \left(\hat{I}-\sum_{j=1}^{N^{\sigma}}|\phi^{\sigma}_{j}\rangle\langle\phi^{\sigma}_{j}|\right) \times(v_{H}+V^{\sigma}_{x}-v_{Hx})|\phi^{\sigma}_{i}\rangle = 0, \quad (7)$$

as this requires only the evaluation of occupied orbitals.

In another publication we introduced the local Fock exchange (LFX) potential, where this potential optimally adopts the HF ground state as its own approximate ground state[5]. Starting with the calculated HF density, this is again accomplished by direction variation of the potential where the change in the potential is given by

$$\delta v^{\sigma}(\mathbf{r}) = \int d\mathbf{r}'\frac{1}{|\mathbf{r}-\mathbf{r}'|}\frac{\delta T_{HF}[v^{\sigma}_{Hx}]}{\delta v^{\sigma}_{Hx}(\mathbf{r}')}. \quad (8)$$

The reason for choosing this is the particularly simple form of the functional derivative

$$\frac{\delta T[v_{Hx}^{\sigma}]}{\delta v_{Hx}^{\sigma}(\mathbf{r})} = \rho_{\mathrm{HF}}(\mathbf{r}) - \rho_v(\mathbf{r}), \tag{9}$$

where it can be seen clearly that at the minimum the HF density, $\rho_{\mathrm{HF}}(\mathbf{r})$ and the LFX density, $\rho_v(\mathbf{r})$ are equal[23]. In the LFX, one obtains the best local potential that replicates the HF density. For a numerical procedure, it was more robust to optimise the LFX potential using a Hartree-like energy of the difference in the densities, so U is minimised, where U is

$$U = \int\int d\mathbf{r}\mathbf{r}' \frac{\left(\rho_{\mathrm{HF}}(\mathbf{r}) - \rho_v(\mathbf{r})\right)\left(\rho_{\mathrm{HF}}(\mathbf{r}') - \rho_v(\mathbf{r}')\right)}{|\mathbf{r} - \mathbf{r}'|}. \tag{10}$$

2. Fractional Occupancies

Implicitly the formulation of the EXX applies only to insulating systems, as it has been assumed that the eigenvalues of the KS system are divided into two kinds; occupied up to the N^{σ}-th orbital and unoccupied thereafter. To allow the application of the KS system to a metallic system each orbital must be assigned an occupancy, n_i^{σ} with values; $0 \leq n_i^{\sigma} \leq 1$. The density is then

$$\rho(\mathbf{r}) = \sum_{i}^{\infty} n_i^{\sigma} \phi_i^{\dagger\sigma}(\mathbf{r})\phi_i^{\sigma}(\mathbf{r}). \tag{11}$$

Quantities such as the kinetic energy are written as

$$T = -\frac{1}{2}\sum_{i}^{\infty} n_i^{\sigma} \int d\mathbf{r}\phi_i^{\dagger\sigma}(\mathbf{r})\nabla^2\phi_i^{\sigma}(\mathbf{r}), \tag{12}$$

and the Fock exchange energy as

$$V_x = -\frac{1}{2}\sum_{\sigma}\sum_{i,j=1}^{\infty} n_i^{\sigma} n_j^{\sigma} \int\int d\mathbf{r}d\mathbf{r}' \frac{\phi_j^{\dagger\sigma}(\mathbf{r})\phi_i^{\sigma}(\mathbf{r})\phi_i^{\dagger\sigma}(\mathbf{r}')\phi_j^{\sigma}(\mathbf{r}')}{|\mathbf{r} - \mathbf{r}'|}. \tag{13}$$

To retain numerical stability the occupancies must vary smoothly from $1 \to 0$ on crossing the Fermi level, hence smearing is used. In the density of states of an insulating system the energy eigenvalues are Dirac δ functions. For a metallic system the delta functions are replaced with a broadening function, δ_θ

$$\varepsilon_i^{\sigma} \to \delta_\theta(\varepsilon_i^{\sigma}) = \frac{1}{\theta}\tilde{\delta}\left(\frac{\varepsilon_i^{\sigma}}{\theta}\right). \tag{14}$$

$\tilde{\delta}(x)$ is the smearing function and integrates to 1, and in the limit $\theta \to 0$ then δ_θ tends to the Dirac δ function. The occupancy of a band is

$$n_i^{\sigma} = \tilde{\Theta}\left(\frac{\varepsilon_F - \varepsilon_i^{\sigma}}{\theta}\right) = \int_{-\infty}^{\frac{\varepsilon_F - \varepsilon_i^{\sigma}}{\theta}} \tilde{\delta}(x)dx, \tag{15}$$

and the Fermi level is then defined by the number of electrons

$$N = \sum_{\sigma}\sum_{i=1}^{\infty} \tilde{\Theta}\left(\frac{\varepsilon_F - \varepsilon_i^{\sigma}}{\theta}\right). \tag{16}$$

3. EXX Extended To Metals

Following the extension of density functional perturbation theory to metals of Baroni *et al*[24], to extend our method for calculating the EXX potential we must introduce fractional occupancies into the functional derivative. Expanding the functional derivative of energy with respect to potential using the chain rule gives

$$\frac{\delta E[v_{Hx}^\sigma]}{\delta v_{Hx}^\sigma(\mathbf{r})} = \sum_{i=1}^{N^\sigma} \int d\mathbf{r}' \frac{\delta E[v_{Hx}^\sigma]}{\delta \phi_i^\sigma(\mathbf{r}')} \frac{\delta \phi_i^\sigma(\mathbf{r}')}{\delta v_{Hx}^\sigma(\mathbf{r})} + \text{h.c.} \tag{17}$$

Also, the derivative of an orbital with respect to the potential can be partitioned

$$\frac{\delta \phi_i^\sigma(\mathbf{r}')}{\delta v_{Hx}^\sigma(\mathbf{r})} = -\sum_{j=1,j\neq i}^{\infty} \frac{\phi_j^\sigma(\mathbf{r})\phi_j^\sigma(\mathbf{r}')}{\varepsilon_j^\sigma - \varepsilon_i^\sigma}\phi_i^\sigma(\mathbf{r}') \tag{18}$$

$$= -\sum_{k=1,k\neq i}^{\infty} n_k^\sigma \frac{\phi_k^\sigma(\mathbf{r})\phi_k^\sigma(\mathbf{r}')}{\varepsilon_k^\sigma - \varepsilon_i^\sigma}\phi_i^\sigma(\mathbf{r}') - \sum_{a=1,a\neq i}^{\infty} (1-n_a^\sigma) \frac{\phi_a^\sigma(\mathbf{r})\phi_a^\sigma(\mathbf{r}')}{\varepsilon_a^\sigma - \varepsilon_i^\sigma}\phi_i^\sigma(\mathbf{r}'). \tag{19}$$

Substitution of (19) into the functional derivative (17) gives

$$\begin{aligned}\frac{\delta E[v_{Hx}^\sigma]}{\delta v_{Hx}^\sigma(\mathbf{r})} = & -\sum_{i=1}^{\infty}\sum_{k=1,k\neq i}^{\infty} n_i^\sigma n_k^\sigma \left[\frac{\phi_k^{\sigma\dagger}(\mathbf{r})\phi_i^\sigma(\mathbf{r})}{\varepsilon_k^\sigma - \varepsilon_i^\sigma}\langle\phi_i^\sigma|v_H + V_x^\sigma - v_{Hx}|\phi_k^\sigma\rangle + \text{h.c.}\right] \\ & -\sum_{i=1}^{\infty}\sum_{a=1,a\neq i}^{\infty} n_i^\sigma(1-n_a^\sigma) \left[\frac{\phi_a^{\sigma\dagger}(\mathbf{r})\phi_i^\sigma(\mathbf{r})}{\varepsilon_a^\sigma - \varepsilon_i^\sigma}\langle\phi_i^\sigma|v_H + V_x^\sigma - v_{Hx}|\phi_a^\sigma\rangle + \text{h.c.}\right] \\ & +\sum_{i=1}^{\infty} \Delta n_i^\sigma(\Delta\varepsilon_F - \Delta\varepsilon_i^\sigma)|\phi_i^\sigma(\mathbf{r})|^2,\end{aligned} \tag{20}$$

where the last term accounts for possible changes in occupation numbers induced by shifts in the eigenvalues, $\Delta\varepsilon_i^\sigma = \langle\phi_i^\sigma|v_H + V_x^\sigma - v_{Hx}|\phi_i^\sigma\rangle$ as well as in the Fermi energy of the system. The first term in equation (20) cancels with its complex conjugate upon interchange of the indices i and k and the second term can be simplified by expansion of the Hermitian conjugate

$$\begin{aligned}\frac{\delta E[v_{Hx}^\sigma]}{\delta v_{Hx}^\sigma(\mathbf{r})} = & -2\sum_{i=1}^{n_i^\sigma\to 0}\sum_{a=1}^{\infty}(n_i^\sigma - n_a^\sigma)\tilde{\Theta}\left(\frac{\varepsilon_a^\sigma - \varepsilon_i^\sigma}{\theta}\right)\frac{\phi_a^{\sigma\dagger}(\mathbf{r})\phi_i^\sigma(\mathbf{r})}{\varepsilon_a^\sigma - \varepsilon_i^\sigma}\langle\phi_i^\sigma|v_H + V_x^\sigma - v_{Hx}|\phi_a^\sigma\rangle \\ & +\sum_{i=1}^{\infty}\Delta n_i^\sigma(\Delta\varepsilon_F - \Delta\varepsilon_i^\sigma)|\phi_i^\sigma(\mathbf{r})|^2.\end{aligned} \tag{21}$$

Θ is introduced and allows the sum over i to be truncated once the occupancy of the i-th state becomes negligible, by exploiting the symmetry in i and a and the relation $\tilde{\Theta}(x)+\tilde{\Theta}(-x) = 1$. The term when $a = i$ can be evaluated as long as; $(n_i^\sigma - n_a^\sigma)/(\varepsilon_a^\sigma - \varepsilon_i^\sigma)$ is replaced with the limit $-\tilde{\delta}((\varepsilon_F^\sigma - \varepsilon_i^\sigma)/\theta)$ whenever $\varepsilon_a^\sigma - \varepsilon_i^\sigma \to 0$, which accounts for the change in the occupancy due to $\Delta\varepsilon_i^\sigma$.

Retaining the structure of the EXX method for insulators we have

$$\frac{\delta E[v_{Hx}^\sigma]}{\delta v_{Hx}^\sigma(\mathbf{r})} = 2\sum_{i=1}^{n_i^\sigma\to 0} n_i^\sigma \tilde{\phi}_i^{\sigma\dagger}(\mathbf{r})\phi_i^\sigma(\mathbf{r})$$

$$+\sum_{i=1}^{\infty}\Delta n_i^\sigma \Delta\varepsilon_F |\phi_i^\sigma(\mathbf{r})|^2. \tag{22}$$

where the first order orbital, $\tilde{\phi}_i^\sigma(\mathbf{r})$ is

$$\begin{aligned}\tilde{\phi}_i^\sigma(\mathbf{r}) = & -\sum_{a=1}^{\infty}\frac{(n_i^\sigma - n_a^\sigma)}{n_i^\sigma}\tilde{\Theta}\left(\frac{\varepsilon_a^\sigma-\varepsilon_i^\sigma}{\theta}\right)\phi_a^\sigma(\mathbf{r}) \\ & \times\frac{\langle\phi_a^\sigma|v_H+V_x^\sigma-v_{Hx}|\phi_i^\sigma\rangle}{\varepsilon_a^\sigma-\varepsilon_i^\sigma}.\end{aligned} \tag{23}$$

To calculate the first order orbital in a tractable manner, the orbital is partitioned into a sum over states with full or partial occupancy and a sum over unoccupied states, thus

$$\begin{aligned}\tilde{\phi}_i^\sigma(\mathbf{r}) = & -\sum_{k=1}^{n_i^\sigma\to 0}\frac{(n_i^\sigma - n_k^\sigma)}{n_i^\sigma}\tilde{\Theta}\left(\frac{\varepsilon_k^\sigma-\varepsilon_i^\sigma}{\theta}\right)\phi_k^\sigma(\mathbf{r})\frac{\langle\phi_k^\sigma|v_H+V_x^\sigma-v_{Hx}|\phi_i^\sigma\rangle}{\varepsilon_a^\sigma-\varepsilon_i^\sigma} \\ & -\sum_{a=n_i^\sigma\to 0}^{\infty}\phi_a^\sigma(\mathbf{r})\frac{\langle\phi_a^\sigma|v_H+V_x^\sigma-v_{Hx}|\phi_i^\sigma\rangle}{\varepsilon_a^\sigma-\varepsilon_i^\sigma}.\end{aligned} \tag{24}$$

While the first term in equation (24) can be directly evaluated using our method in reference [21], we calculate the second term in the above from a Sternheimer equation where the projector

$$P_c = \hat{I} - \sum_{j=1}^{n_j^\sigma\to 0}|\phi_j^\sigma\rangle\langle\phi_j^\sigma|. \tag{25}$$

in the Sternheimer equation projects all states with partial or full occupancy.

It is straightforward to show that for a system of non-partial occupancy the definitions of the functional derivative and first order orbital revert to the forms given for insulators.

4. LFX Extended To Metals

Here the LFX potential is extend to metallic systems along similar lines. The LFX functional derivative is simply the difference of two densities

$$\begin{aligned}\frac{\delta T_{\rm HF}[v_{Hx}^\sigma]}{\delta v_{Hx}^\sigma(\mathbf{r})} &= \rho_{\rm HF}^\sigma(\mathbf{r}) - \rho_v^\sigma(\mathbf{r}) \\ &= \sum_{i=1}^{n_{i,\rm HF}^\sigma\to 0} n_{i,\rm HF}^\sigma \psi_i^{\sigma\dagger}(\mathbf{r})\psi_i^\sigma(\mathbf{r}) - \sum_{i=1}^{n_i^\sigma\to 0} n_i^\sigma\phi_i^{\sigma\dagger}(\mathbf{r})\phi_i^\sigma(\mathbf{r}),\end{aligned} \tag{26}$$

where $\rho_{\rm HF}^\sigma$ is the Hartree-Fock density and ρ_v^σ is the density of LFX Kohn-Sham system. As in the case of insulators, the objective functional, $U[v_{Hx}^\sigma]$ is given by

$$U[v_{Hx}^\sigma] = \int\int d\mathbf{r}d\mathbf{r}'\frac{[\rho_{\rm HF}^\sigma(\mathbf{r})-\rho_v^\sigma(\mathbf{r})][\rho_{\rm HF}^\sigma(\mathbf{r}')-\rho_v^\sigma(\mathbf{r}')]}{|\mathbf{r}-\mathbf{r}'|}. \tag{27}$$

5. Implementation

Our procedure for determining the EXX and LFX potentials involves a direct minimisation of the potential, using the optimisation schemes outlined in references

[21] and [5]. For the EXX potential we perform an LDA calculation (exchange and correlation) to give an initial approximate effective potential. For the LFX potential we are required to perform a HF calculation to generate the target density. The variation of the potential is accomplished via a conjugate gradient scheme using a line search. We use a Fletcher-Reeves[25] conjugate gradient update with a parabolic line search to minimise our objective functionals (the HF total energy or U). After each step of this minimisation new Kohn-Sham orbitals are found non-self-consistently and the occupancies corresponding to these new orbitals updated. When the difference in the objective functional per step is smaller than a predetermined limit the calculation is considered converged.

EXX and LFX has been implemented with the pseudopotential plane-wave code CASTEP[26, 27]. The orbitals, density and potentials are represented on rectilinear grids in the usual manner of a plane-wave implementation[28]. Kohn-Sham orbitals are described on reciprocal space grid points $\mathbf{G}$ within a sphere of radius G_{max}, and the density and potentials are described with a sphere of radius $2G_{max}$. Hence the grids in both real and reciprocal space used to represent the density and potentials have twice the dimensions of the grids used for the orbitals. The minimisation of the potentials is performed in real space by direct variation.

The pseudopotentials used in this work are the optimised norm-conserving pseudopotentials generated using the OPIUM code[29]. As we are attempting to treat exchange exactly for the valence electrons, we use the HF approximation to generate the pseudopotentials. The non-analytic behaviour of HF for pseudopotentials is treated by using the localisation and optimisation scheme of Al-Shadi *et al.*[30] and we include semi-core states as valence in all cases where applicable. In the calculations that follow, the basis set size (plane-wave cut off energy) and Brillouin-zone sampling were chosen to be less than 2.5 meV/atom. Sampling of the Brillouin-zone is accomplished using a Monkhorst-Pack grid[31] of $12 \times 12 \times 12$.

6. Calculated Electronic Structures

The EXX and LFX potentials were applied to some elemental metallic systems and the band structures plotted. We also include calculated LDA and HF band structures for comparison. The total energy differences for the EXX and LFX from the corresponding HF total energies are shown in Table 1. In all cases we use the HF total energy expression in terms of the partially-occupied orbitals of the corresponding potential. In all cases the EXX and LFX total energies are nearly identical and minimally above the HF result. Using orbitals non-self-consistently generated from other functionals will give a larger energy difference[14, 32].

It is well known that the Hartree-Fock approximation, when applied to jellium, gives at the Fermi level a logarithmically divergent dispersion, hence the density of states vanishes at the Fermi level. The divergence in the Hartree-Fock calculation can be seen in figure 1, however by using the local potentials, LFX and EXX, both give band

Material	ΔE (eV)	
	EXX	LFX
Jellium	0.003	0.003
Na	0.009	0.009
Mg	0.057	0.058
Al	0.036	0.036
Ca	0.298	0.314
Graphene	0.110	0.110

Table 1. Total energy differences from the HF total energy for EXX and LFX.

structures matching the LDA (considered exact) results for the homogeneous electron gas.

Moving away from the ideal situation of the homogeneous electron gas and looking at a real material, for example sodium (figure 2), HF gives a greatly increased valence bandwidth, with a steep (vertical) dispersion at the Fermi level, and EXX and LFX give band structures very close to the LDA result. The same observations as made for sodium are made for magnesium and aluminium band structures and hence are not shown.

For calcium the result is more dramatic with HF giving an insulating ground state, yet using the EXX and LFX the result is metallic and accurately reproduces the Ca LDA band structure. The EXX and LFX are similar to the LDA band structure result.

Finally, for a different class of metallic material, we have calculated the result for graphene. Encouragingly, the LDA, EXX and LFX methods are very similar, and as expected, HF forces open a gap at the K-point giving an insulating state.

In the literature (and textbooks)[33, 34], the failure of HF to correctly describe jellium as a metal is attributed to the lack of correlation and it is often claimed that only by including correlation can the incorrect treatment of metals by HF be rectified. The effect of correlation is to "screen" the exchange interaction, removing the divergence at the Fermi level. However the EXX and LFX methods are exchange-only methods but from the calculations it is evident that the divergence (or steep slope of the dispersion curve) vanishes when using a local potential. Hence the divergence is an artifact of the non-local exchange potential used in Hartree-Fock rather than lack of correlation[2]. In Hartree-Fock, the self-repulsion in the unoccupied states is not canceled resulting in the very large band gaps seen in insulators. This repulsion pushes the virtual states to higher energies, diminishing the density of states at the Fermi level.

7. Conclusions

EXX and LFX give a good description of metals in contrast to the poor description that results from using HF. This is particularly striking for LFX, which uses the HF density from a HF calculation that gives qualitatively the wrong result. The EXX and

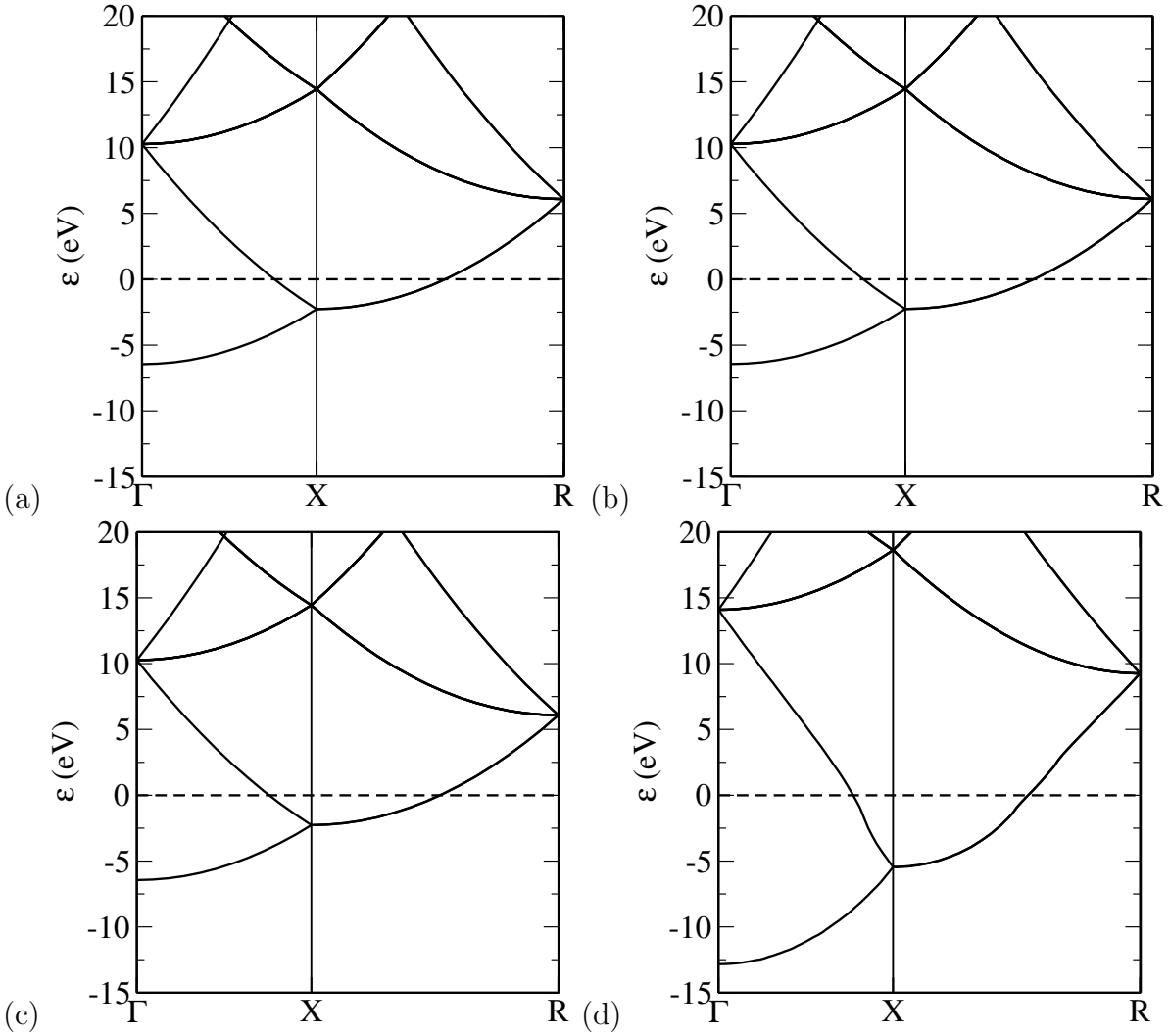

Figure 1. Band structures for jellium using the following potentials; (a) LDA, (b) EXX, (c) LFX and (d) HF. The Fermi level has been set to 0eV for all band structures.

LFX band structures for simple metals coincide (almost) with the LDA band structures, the EXX/LFX total energies neglect correlation and differ substantially from the LDA total energy. Neither EXX or LFX display the unphysical divergence at the Fermi level seen in some Hartree-Fock calculations and both correctly give metallic states when HF gives insulating (calcium and graphene). An advantage of the methods presented here over HF based methods is that a single technique for dealing with exact exchange can be used across a wide variety of systems from metals to insulators.

References

[1] E. R. Davidson, *Rev. Mod. Phys.* **44**, 451 (1972).
[2] A.I. Blair, A. Kroukis, N.I. Gidopoulos, *J. Chem. Phys* **142**, 084116 (2015).
[3] N. I. Gidopoulos, P. G. Papaconstantinou, and E. K. U. Gross, *Phys. Rev. Lett.* **88**, 033003 (2002).
[4] E. Ospadov, I. G. Ryabinkin and V. N. Staroverov. *J. Chem. Phys* **146**, 084103 (2017).

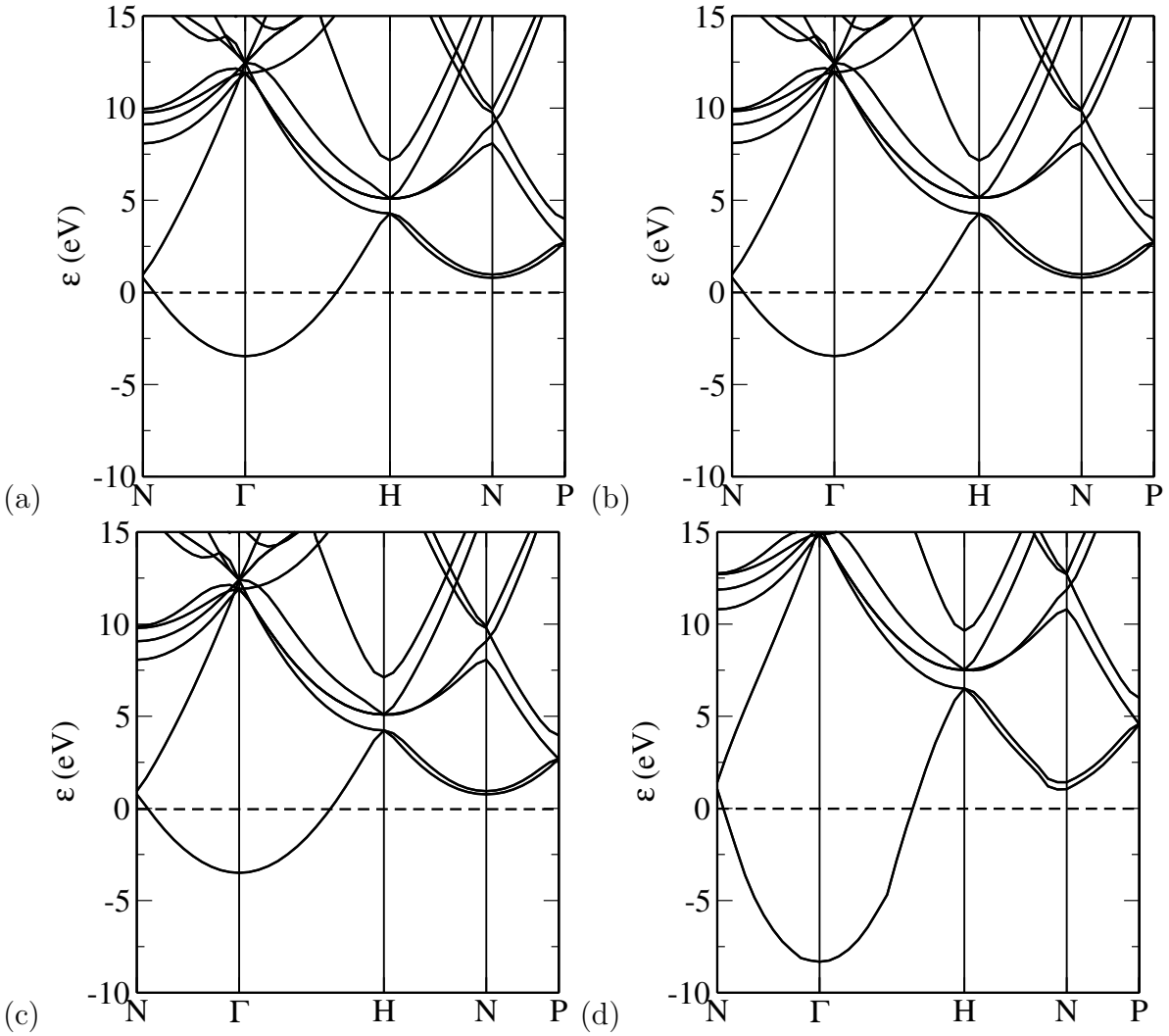

Figure 2. Band structures for sodium using the following potentials; (a) LDA, (b) EXX, (c) LFX and (d) HF. The Fermi level has been set to 0eV for all band structures.

[5] T. W. Hollins, S. J. Clark, S. J. Refson and N. I. Gidopoulos, *J. Phys. Condens. Matter* **29**, 04LT01 (2017).

[6] S. Kummel and L. Kronik, *Rev. Mod. Phys* **80**, 3 (2008)

[7] A. Hesselmann, A. W. Gotz, F. Della Sala, and A. Görling, *J. Chem. Phys* **127**, 054102 (2007).

[8] M. Betzinger, C. Friedrich, A. Görling and S. Bluegel, *Phys. Rev. B* **85**, 245124 (2012).

[9] A. Hesselmann and A. Görling *Chem. Phys. Lett* **455**, 110 (2008).

[10] M. Betzinger, C. Friedrich, S. Blugel and A. Görling *Phys. Rev B* **83**, 045105 (2011).

[11] D. Kodderitzsch, H. Ebert, H. Akai and E. Engel, *J. Phys. Condens. Matter* **21**, 064208 (2009).

[12] H. Jiang and E. Engel, *J. Chem. Phys.* **123**, 224102 (2005).

[13] E. Engel and H. Jiang *Int. J. Quantum Chem.* **106**, 3242 (2006).

[14] F. Tran, P. Blaha, M. Betzinger and S. Bluegel, *Phys. Rev. B* **91**, 165121 (2015).

[15] M. Stadele, J. A. Majewski, P. Vogl and A. Görling, *Phys. Rev. Lett.* **79**, 2089 (1997).

[16] N. Gidopoulos and N. N. Lathiotakis, *Advances in Atomic, Molecular and Optical Physics* **64**, Chapter 6, Elsevier (2015)

[17] N. Gidopoulos and N N ,Lathiotakis, *J. Chem. Phys.* **136**, 224109 (2012).

[18] T. Kotani and H. Akai, *Phys. Rev. B* **52**, 17153 (1995).

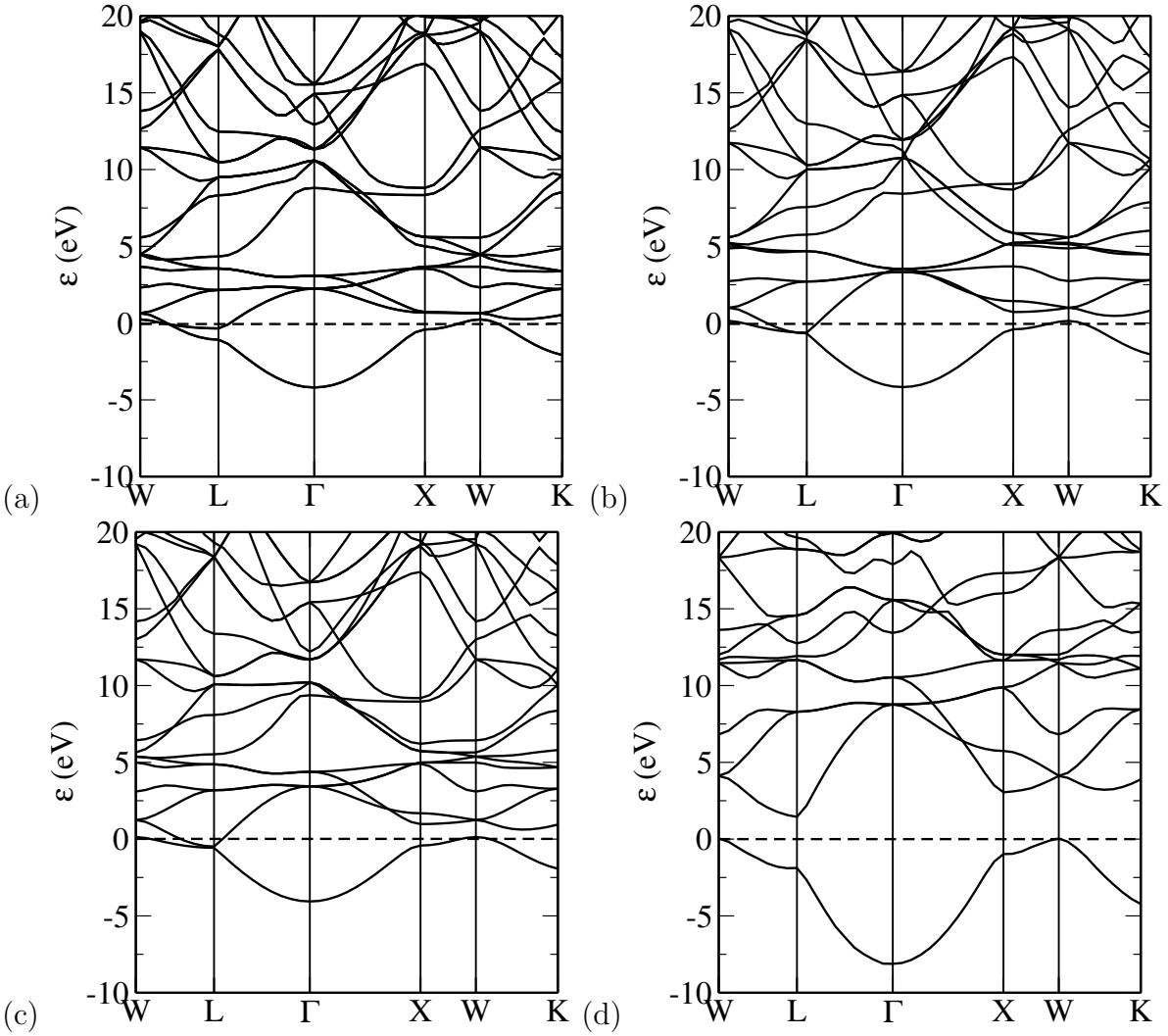

Figure 3. Band structures for calcium using the following potentials; (a) LDA, (b) EXX, (c) LFX and (d) HF. The Fermi level has been set to 0eV for all band structures.

[19] T. Kotani and H. Akai *Physica B* **237**, 332 (1997).
[20] T. Kotani *J. Phys. Condens. Matter* **10**, 9241 (1998).
[21] T. W. Hollins, S. J. Clark, S. J. Refson and N. I. Gidopoulos, *Phys. Rev. B* **85**, 235126 (2012).
[22] J. Harl, L. Schimka and G. Kresse, *Phys. Rev. B* **81**, 115126 (2010).
[23] N. I. Gidopolous, *Phys. Rev. A* **83**, 040502(R) (2011).
[24] S. Baroni, S. de Gironcoli and A. Dal Corso, *Rev. Mod. Phys.* **73**, 515 (2001).
[25] R. Fletcher and C. M. Reeves, *Comput. J.* **7** (1964).
[26] S. J. Clark, M. D. Segall, C. J. Pickard, P. J. Hasnip, M. J. Probert, K. Refson, M. C Payne, MC, *Z. fur Krist.*, **220** 567 (2005)
[27] M. D. Segall, P. J. D. Lindan, M. J. Probert, C. J. Pickard, P. J. Hasnip, S. J. Clark, M. C. Payne, *J. Phys. Condens. Matter* **14**, 2717 (2002).
[28] R. Car and M. Parrinello, *Phys. Rev. Lett.* **55**, 2471 (1985).
[29] A. M. Rappe, K. M. Rabe, E. Kaxiras, and J. D. Joannopoulos *Phys. Rev. B* **41** 1227(R) (1991).
[30] W. A. Al-Saidi, E. J. Walter, and A. M. Rappe, *Phys. Rev. B* **77** 075112 (2008).
[31] H. J. Monkhorst and J. D. Pack *Phys. Rev. B* **13** 5188 (1976).
[32] F. Tran, P. Blaha, M. Betzinger and S. Bluegel, *Phys. Rev. B* **94**, 165149 (2016).

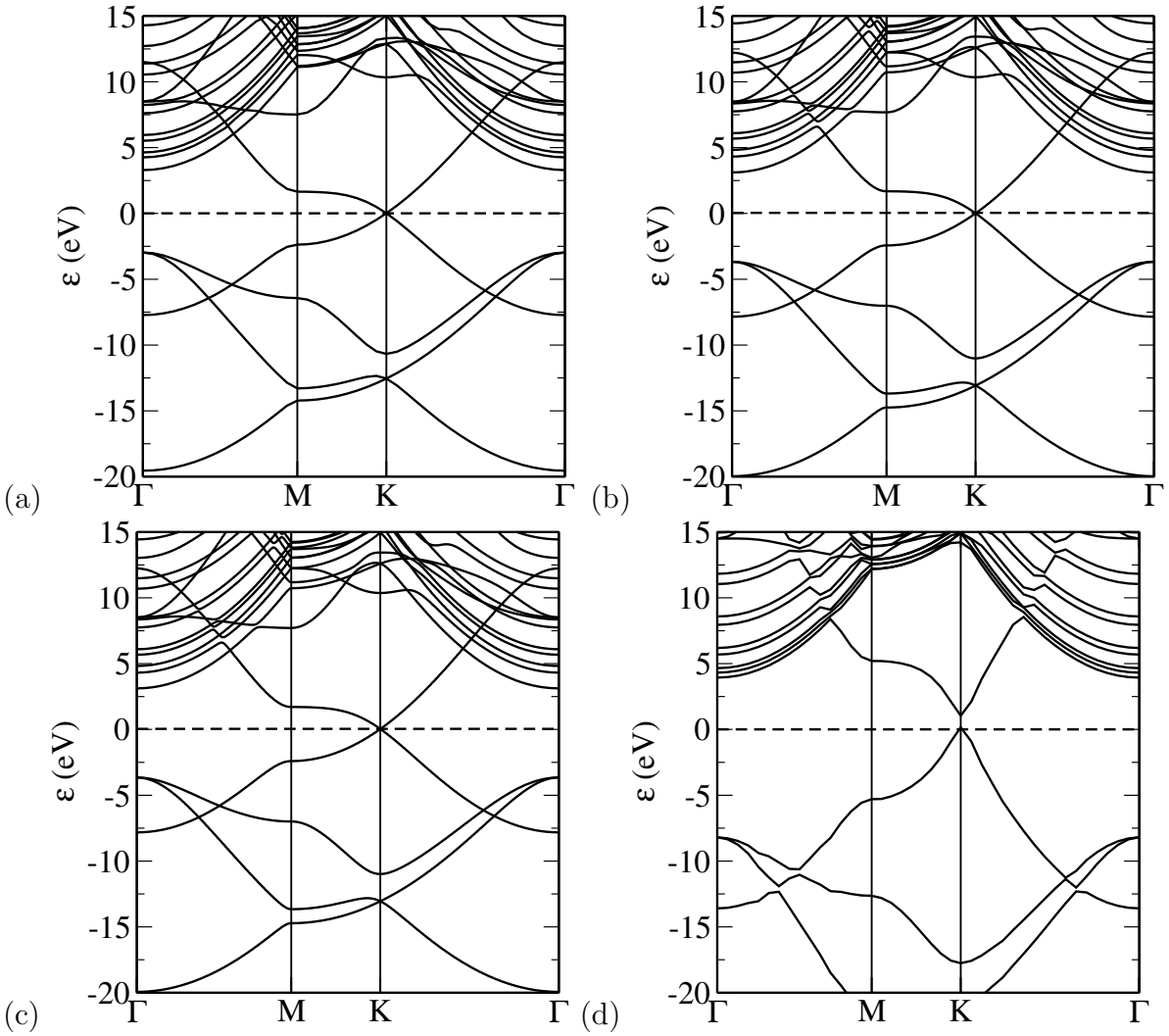

Figure 4. Band structures for graphene using the following potentials; (a) LDA, (b) EXX, (c) LFX and (d) HF. The Fermi level has been set to 0eV for all band structures.

[33] N. W. Ashcroft and N. D. Mermin, "Solid state physics", Harcourt Publishers (1976).
[34] J. C. Inkson, "Many-body theory of solids", Springer, Plenum Press NY, (1984).